2024 IEEE International Conference on Robotics and Automation (ICRA 2024)
May 13-17, 2024. Yokohama, Japan

Particle Filter with Stable Embedding for State Estimation of the Rigid Body Attitude System on the Set of Unit Quaternions

Hee-Deok Jang, Jae-Hyeon Park, and Dong Eui Chang*

***Abstract*— This paper presents a novel method for state estimation of rigid body attitude system evolving on the manifold S^3, which is crucial in robotics and drone applications. We introduce a particle filter with stable embedding that extends the system into Euclidean space while ensuring stability of the manifold. Our particle filter with stable embedding enables accurate state estimation by maintaining estimated state values in close proximity to the manifold, while requiring significantly fewer computational resources than the standard exponential-map-based method that keeps state estimates on the manifold. Furthermore, our method facilitates the application of usual techniques designed for particle filters in Euclidean spaces, to the manifold system, as is, without any modification. The accuracy and the efficiency of our particle filter are confirmed both by simulation and by real drone experiments.**

***Index Terms*— Stable embedding, manifold, particle filter, attitude estimation.**

I. INTRODUCTION

The accurate estimation of the state of a rigid body attitude system evolving over time is essential for robotics and control applications [1], [2], [3], [4], [5]. To address this need, state estimation filters grounded in Bayesian principles have emerged as key tools, including the extended Kalman filter (EKF), unscented Kalman filter (UKF), and particle filter. The particle filter is particularly advantageous for nonlinear and non-Gaussian dynamical systems due to its representation of the state using a finite number of particles, composed of samples and associated weights. However, directly applying a standard particle filter designed in Euclidean space to estimate the state of a rigid body system defined on a manifold, such as the set, $SO(3)$, of rotation matrices or the set, S^3, of unit quaternions, often results in inaccuracies and divergence. This is attributed to the inherent limitations of the standard particle filter in addressing geometric filtering challenges, causing the estimated state during the filtering process to deviate from the defined manifolds due to non-closure under the addition or subtraction operation. To address these challenges, various studies on particle filters for systems defined on manifolds are ongoing.

Chiuso and Soatto [6] first introduced a particle filter for state estimation of systems on Lie groups. They estimated the random walk for state changes using the properties of Lie algebra and utilized a discrete-time framework that employs exponential map from Lie algebra to Lie group to ensure the state remains on the Lie group. Kwon et al. [7] applied the particle filter by Liu and West [8] to a system defined on $SE(3)$ and employed first-order exponential Euler discretization to maintain the state on $SE(3)$. Similarly, Choi and Christensen [9] introduced a particle filter for 3D visual tracking defined on $SE(3)$ using first-order exponential Euler discretization. Zhang et al. [10] extended the feedback particle filter devised in Euclidean space [11] to Riemannian manifolds and matrix Lie groups, utilizing the exponential map to confine the particles to the manifold. Marjanovic and Solo [12] developed a general particle filter for matrix Lie groups, accommodating general stochastic differential equations for state dynamics. They employed an exponential map based on [13] to derive a discrete-time formulation that ensures particles remain on the manifold. In a subsequent work [14], the particle filter of [12] was extended to the Stiefel manifold, and an exponential map was also used. Snoussi and Mohammad-Djafari [15] proposed a particle filter for systems defined on Riemannian manifolds, connecting samples generated in the tangent space with particles on the manifold using an exponential map. These particle filters commonly use the exponential maps to preserve manifold structure but are computationally expensive [2], [3].

In this paper, we introduce a method for applying the standard particle filter developed in Euclidean space to estimate accurately and efficiently the state of a rigid body attitude system defined on S^3, where $S^3 = \{q \in \mathbb{H} | \|q\| = 1\}$, where $\mathbb{H}$ denotes the set of quaternions which is isomorphic, as a vector space, to $\mathbb{R}^4$. We achieve this using a stable embedding technique [16]. This state estimation technique, based on stable embedding, has previously been successfully applied to both EKF [2] and UKF [3], resulting in computationally efficient and highly accurate filters. With the stable embedding approach, for a dynamical system defined on a manifold, we embed the manifold into Euclidean space and extend the system accordingly. Then, we modify the extended system to ensure that the manifold becomes an invariant attractor of the resultant system. The use of low computational cost discretization techniques commonly used in Euclidean space is possible due to the extension of the modified system to Euclidean space, which contrasts previous studies using Lie groups and/or exponential maps. Furthermore, the stability property conferred by stable embedding ensures that the state estimated by the derived discrete-time dynamic system remains close to the manifold,

* Corresponding author

This work was in part supported by the CARAI grant funded by DAPA and ADD (No. UD190031RD), by IITP (No. 2022-0-00469, No. 20210005900012003), by NRF (No. 2021R1A2C2010585) and by BK21 Program.

The authors are with the School of Electrical Engineering, Korea Advanced Institute of Science Technology, Daejeon, Korea. {jhd6844, alchemiclove, dechang}@kaist.ac.kr

resulting in high estimation accuracy. We evaluate the performance of our proposed particle filter, which incorporates stable embedding, by conducting simulations and real drone experiments. A significant advantage of our filter is its ability to maintain state estimates in close proximity to the manifold while incurring only a minimal increase in computational demand. In particle filter-based state estimation, computational requirements have a direct influence on the number of particles that can be employed. Consequently, having greater computational capacity opens up opportunities for exploring state estimation of complex systems and the application of additional techniques to enhance performance.

The structure of the paper is organized as follows. Section II introduces our particle filtering method for a rigid body system, utilizing stable embedding. Section III demonstrates the performance of our proposed method with simulation and real drone experiments. Lastly, Section IV offers the conclusion.

II. MAIN METHOD

A. Rigid Body System with Stable Embedding

The rigid body kinematics is given as follows:

$$\dot{q} = \frac{1}{2} q\Omega, \tag{1}$$

where $q = (q_0, q_1, q_2, q_3) \in \mathrm{S}^3$ is the attitude, and $\Omega \in \mathbb{R}^3$ is the body angular velocity. In (1), $\Omega \in \mathbb{R}^3 \approx 0 \times \mathbb{R}^3 \subset \mathbb{H}$ is considered as an imaginary quaternion, and $q\Omega$ denotes quaternion multiplication between q and Ω. The rotation matrix corresponding to q is given by

$$R(q) = \begin{bmatrix} 2q_0^2 + 2q_1^2 - 1 & 2(q_1q_2 - q_0q_3) & 2(q_1q_3 + q_0q_2) \\ 2(q_1q_2 + q_0q_3) & 2q_0^2 + 2q_2^2 - 1 & 2(q_2q_3 - q_0q_1) \\ 2(q_1q_3 - q_0q_2) & 2(q_2q_3 - q_0q_1) & 2q_0^2 + 2q_3^2 - 1 \end{bmatrix}.$$

The measurement model is given as follows:

$$z = R(q)^T e_3 + n, \tag{2}$$

where $z \in \mathbb{R}^3$ is the accelerometer unit measurement in the absence of translational motion, $e_3 = (0, 0, 1) \in \mathbb{R}^3$, and $n \sim \mathcal{N}(0, N_C) \in \mathbb{R}^3$ is measurement noise, with $\mathcal{N}(\mu, \Sigma)$ denoting Gaussian noise with mean μ and covariance Σ.

We extend the system (1) from S^3 to $\mathbb{H}$, treating q as an element of $\mathbb{H}$, and define a function $V : \mathbb{H} \to \mathbb{R}_{\geq 0}$ as

$$V(q) = \frac{1}{4}\left(\|q\|^2 - 1\right)^2,$$

where $\|\cdot\|$ is the norm defined as $\|q\| = \sqrt{q_0^2 + q_1^2 + q_2^2 + q_3^2}$. The function V satisfies $V(q) = 0, \forall q \in \mathrm{S}^3$ and its derivative, which is given as $\nabla V = (\|q\|^2 - 1)q$, satisfies $\langle \nabla V, \frac{1}{2} q\Omega \rangle = 0$ for all $q \in \mathbb{H}$ and $\Omega \in \mathbb{R}^3$, where $\langle \cdot, \cdot \rangle$ is the Euclidean inner product on $\mathbb{H} \approx \mathbb{R}^4$. We modify the extended system defined on $\mathbb{H}$ by adding $-\alpha \nabla V$ as follows:

$$\dot{q} = \frac{1}{2} q\Omega - \alpha\left(\|q\|^2 - 1\right) q, \tag{3}$$

where $\alpha > 0$ is a constant. It is easy to demonstrate that the modified system (3) is identical to the original system (1) when restricted to S^3, as per the definition of S^3. Along any trajectory of (3), $\frac{d}{dt} V = \langle \nabla V, \frac{1}{2} q\Omega - \alpha \nabla V \rangle = -\alpha ||\nabla V||^2 \leq 0$. Since V attains its minimum value, 0, on S^3, S^3 can be shown to be exponentially stable [1]. Namely, all trajectories of (3) staring in a neighborhood of S^3 converge to S^3 as t tends to infinity. More detailed mathematical explanations are provided in [1], [16].

Since the system (3) is defined in Euclidean space, we can employ noise modeling and discretization techniques commonly used in Euclidean space. Consider a stochastic dynamical system based on (3) by introducing a noise term and a measurement model (2), as follows:

$$\dot{q} = \frac{1}{2} q\Omega - \alpha\left(\|q\|^2 - 1\right) q + m, \tag{4a}$$

$$z = R(q)^T e_3 + n, \tag{4b}$$

where $m \sim \mathcal{N}(0, M_C) \in \mathbb{H}$ is a process noise. To discretize the system (4), we apply Euler's discretization method with time step $\Delta t > 0$ as follows:

$$q_{k+1} = q_k + \Delta t \left(\frac{1}{2} q_k \Omega_k - \alpha\left(\|q_k\|^2 - 1\right) q_k \right) + m_k, \tag{5a}$$

$$z_k = R(q_k)^T e_3 + n_k, \tag{5b}$$

where $q_k = q(k\Delta t)$, $\Omega_k = \Omega(k\Delta t)$, $z_k = z(k\Delta t)$, $m_k \sim \mathcal{N}(0, M_C \Delta t) \in \mathbb{H}$ and $n_k \sim \mathcal{N}(0, N_D) \in \mathbb{R}^3$, $N_D = N_C/\Delta t$. It's important to ensure that the magnitudes of α and Δt satisfy the condition $0 < \alpha \Delta t < \frac{2}{3}$ for the stability of S^3 under this discretization, as proven in [3].

B. Particle Filter with Stable Embedding

We apply the sampling importance resampling (SIR) filter [17], which is commonly used as the standard particle filter designed in Euclidean space, to the system (5). We term this approach as the particle filter with stable embedding (PF-SE). Since the system (5) is defined in Euclidean space, PF-SE directly employs filtering techniques designed for Euclidean space, including particle initialization and state estimation from particles, without the need for geometric transformations.

First, we generate initial samples q_0^i and the associated weights w_0^i according to the given initial state q_0 as follows: $q_0^i \sim \mathcal{N}(q_0, V) \in \mathbb{H}$, $w_0^i = \frac{1}{N}$ for $i = 1, \ldots, N$, where N is the number of particles, and V is the covariance matrix of the initial state. The initial probability density function is considered as a Gaussian probability density function.

In the particle prediction step, we calculate the particles at the next time step based on the motion model of the system, which describes how particles at the previous time step move based on input. We use the derived discrete-time system (5a) to generate the particles at the next step as:

$$q_{k+1}^i = q_k^i + \Delta t \left(\frac{1}{2} q_k^i \Omega_k - \alpha\left(\|q_k^i\|^2 - 1\right) q_k^i \right) + m_k^i, \tag{6}$$

$i = 1, \ldots, N$, where $m_k^i \sim \mathcal{N}(0, M_C \Delta t)$ is a process noise.

If the standard particle filter is directly applied to (1), the prediction equation is derived using Gaussian noise and Euler discretization methods. However, this approach does not

preserve the geometric properties of S^3, where the particles should ideally lie. Consequently, the particles deviate from S^3, resulting in inaccurate state estimation. To maintain the geometric properties of the particles, a discretization equation for particle prediction can be considered using exponential mapping, as seen in the previous studies on manifold particle filters [7], [9], [10]. Nonetheless, these methods often demand substantial computational resources. Given that particle prediction is performed for all particles, the increased time required for particle prediction multiplies by the total number of particles, which can significantly impact the overall runtime. For systems requiring numerous particles or real-time state estimation, this increase can pose a substantial challenge. In contrast to previous approaches, particle prediction using stable embedding offers the advantage of keeping particles in close proximity to S^3 with only a small amount of computational increase through the computation of the $-\alpha\nabla V$ term.

After the prediction step, we update the weight w_k^i of each particle to w_{k+1}^i using the measurement z_{k+1} and likelihood $p(z_{k+1}|q_{k+1}^i)$. The calculation of w_{k+1}^i through the likelihood obtained from (5b) is as follows:

$$w_{k+1}^i = \frac{p\left(z_{k+1}|q_{k+1}^i\right)}{\sum_{i=1}^N p\left(z_{k+1}|q_{k+1}^i\right)}, \tag{7a}$$

$$p(z_{k+1}|q_{k+1}^i) \propto e^{\frac{1}{2}\left(z_{k+1}-h(q_{k+1}^i)\right)^T N_D^{-1}\left(z_{k+1}-h(q_{k+1}^i)\right)}, \tag{7b}$$

where $h(q) = R(q)^T e_3$. The particles are then resampled according to these weights using systematic resampling, which a commonly employed technique in particle filtering [18]. Resampling is performed at every step. While we chose the systematic resampling method for its ease of implementation, it's worth noting that other particle resampling methods are also available [19], [20].

At the end of every step, we estimate the state at time step $k+1$ as follows:

$$\hat{q}_{k+1} = \sum_{i=1}^N w_{k+1}^i q_{k+1}^i. \tag{8}$$

Since we have embedded the system into Euclidean space by stable embedding, we can calculate the estimation value using a weighted sum, as shown in equation (8). In the previous studies, as S^3 is not closed under addition and subtraction, various methods have been employed to ensure that the average of particles lies on S^3, such as empirical average [21] and Karcher average [22], [23]. Algorithm 1 summarizes the workflow of PF-SE.

Algorithm 1 PF-SE for attitude estimation

Initialization: Sample initial particles $\{q_0^i, w_0^i\}_{i=1}^N$
for $i = 1:N$ **do**
  draw sample $q_0^i \sim \mathcal{N}(q_0, V)$
  initialize weight $w_0^i = \frac{1}{N}$
end for

Iteration: from k to $k+1$
for $i = 1:N$ **do**
  predict particles $q_{k+1}^i \sim p\left(q_{k+1}|q_k^i, \Omega_k\right)$ using (6)
  update weights w_{k+1}^i using (7a) and (7b)
end for
resampling using systematic resampling [18]:
$\left[\{q_{k+1}^i, w_{k+1}^i\}_{i=1}^N\right]$ = resample $\left[\{q_{k+1}^i, w_{k+1}^i\}_{i=1}^N\right]$
state estimation $\hat{q}_{k+1}$ using (8)

III. EXPERIMENTS

We conduct two types of experiments for rigid body attitude estimation. The first experiment is implemented through simulation, and the second one is implemented with data collected with a real drone. We assess the performance using the following four metrics:

$$\hat{e}_k = \frac{1}{J}\sum_{j=1}^J e_k^{(j)}, \qquad [\hat{e}_k] = \frac{1}{K}\sum_{k=0}^K \hat{e}_k,$$

$$\hat{d}_k = \frac{1}{J}\sum_{j=1}^J \left|\|\hat{q}_k^{(j)}\| - 1\right|, \qquad \left[\hat{d}_k\right] = \frac{1}{K}\sum_{k=0}^K \hat{d}_k,$$

where J is the number of trials per experiment, K is the total number of time steps per experiment, and $e_k^{(j)} = \|q_k^{(j)} - \hat{q}_k^{(j)}\|$ represents the norm of the error in attitude estimation at time step k of the j-th trial. The metric $\hat{d}_k$ represents how far the estimated state is from S^3 as the average across all trials.

In both experiments, we consider the following filters for comparison:

- PF : the standard particle filter with the system (1), treating the state as in $\mathbb{H}$ and employing Euler's discretization method and a process noise in $\mathbb{H}$.
- PF-SE : our proposed particle filter with the system (5) with $\alpha = 10$.
- PF-ε : this particle filter uses a closed-form formula for the exponential map, as described in [24], ensuring that particles remain on S^3. The particle prediction is given by

$$q_{k+1}^i = q_k^i \left(\cos\left(\|\Delta v_k^i\|/2\right), \frac{\Delta v_k^i}{\|\Delta v_k^i\|}\sin\left(\|\Delta v_k^i\|/2\right)\right), \tag{9}$$

  where $\Delta v_k^i = \Omega_k \Delta t + \tilde{m}_k^i$ and $\tilde{m}_k^i \sim \mathcal{N}(0, \tilde{M}_C \Delta t) \in \mathbb{R}^3$. The empirical mean of the particles is computed as the normalized eigenvector of the 4×4 matrix $Q = \sum_{i=1}^N w_k^i q_k^i q_k^{i\,T}$ corresponding to its largest eigenvalue [21].

Our contribution primarily lies in the utilization of the system (5), obtained by stable embedding. To effectively demonstrate the superiority of our approach, we maintain consistent workflows for all the three types of filters, including weights update and resampling methods.

For particle initialization, the initial particles of PF-ε

$\{q_0^i\}_{i=1}^N$ are drawn as follows:

$$q_0^i = \tilde{q}_0 \left(\cos\left(\|v^i\|/2\right), \frac{v^i}{\|v^i\|} \sin\left(\|v^i\|/2\right) \right) \tag{10}$$

where $\{v^i\}_{i=1}^N$ are sampled from the Gaussian distribution $\mathcal{N}(0, \tilde{V}) \in \mathbb{R}^3$, and $\tilde{q}_0 \in \mathrm{S}^3$ is the noise-applied initial state that is generated using $v_0 \sim \mathcal{N}(0, \tilde{V}_0) \in \mathbb{R}^3$ and the given initial state $q_0 \in \mathrm{S}^3$ instead of v^i and $\tilde{q}_0$, respectively, following the same procedure as (10). The initial particles of PF and PF-SE are generated as $q_0^i = \tilde{q}_0 + \tilde{q}_0 v^i$, considering $v^i \in \mathbb{R}^3 \approx 0 \times \mathbb{R}^3 \subset \mathbb{H}$, and $\{v^i\}_{i=1}^N$ is consistent across all filters for each trial.

A. Simulation

The configuration parameters are chosen as follows: $q_0 = (1,0,0,0), \tilde{V} = 10^{-4} I_3, \tilde{V}_0 = 10^{-2} I_3, \tilde{M}_C = 10^{-6} I_3, M_C = 10^{-6} I_4, N_C = 10^{-1} I_3, N = 100, J = 100, \Delta t = 0.01, K = 500$. The model for the angular velocity is from [25]:

$$\Omega(t) = \left(\sin\left(\frac{2\pi}{15}t\right), -\sin\left(\frac{2\pi}{18}t + \frac{\pi}{20}\right), \cos\left(\frac{2\pi}{17}t\right) \right).$$

In Fig. 1(a), we observe $\hat{e}_k$ for each filter as the number of steps increases. Initially, all filters exhibit similar error levels. However, as the number of steps increases, both PF-SE and PF-ε maintain low error levels, whereas the error in PF gradually escalates. To gain insights into the increasing $\hat{e}_k$ observed in PF, we turn to Fig. 1(b). At the outset, all filters are in close proximity to S^3. However, as the number of steps increases, PF gradually drifts further away from the manifold, while PF-SE remains closely associated with it. Notably, since PF-SE operates similarly to PF except for the $-\nabla V$ term, we confirm that the stable embedding facilitates convergence to S^3 and enables accurate state estimation.

Table I presents $[\hat{e}_k]$, $\left[\hat{d}_k\right]$, and the average computation time per iterative step for the three filters. PF-SE exhibits the lowest $[\hat{e}_k]$ among the filters, demonstrating its capability of accurate state estimation. Furthermore, PF-SE maintains a distance value approximately 101.49 times lower than PF, underscoring its ability to keep estimated values in close proximity to S^3 due to stable embedding. PF-ε achieves the lowest $\left[\hat{d}_k\right]$ value, thanks to the explicit formula in (9) and the empirical mean. However, this advantage comes at the cost of increased computation time. In terms of computation time, PF requires the least computational resources, as no special techniques are applied to preserve the structure of the manifold, S^3. In contrast, PF-SE and PF-ε exhibit computational increases by a factor of 1.04 and 2.51, respectively, compared to that for PF. Notably, PF-SE not only provides highly accurate state estimation, as evidenced by its lowest $[\hat{e}_k]$, but also offers an efficient computational method with a modest increase in computation time while staying close to S^3. It follows that PF-SE is the best particle filter among the three filters for the rigid body system on S^3.

B. Drone Attitude Estimation: A Real Experiment

In order to analyze the performance of the filters in real environments, we conduct an experiment with a real drone. The drone is controlled by Pixhawk, and accelerometer and gyroscope values are obtained from an IMU sensor in Pixhawk. In addition, since the measurement model (2) requires assumptions that there is no translational motion, the drone is tied to the FFT-GYRO 450 made by EUREKA Dynamics, allowing only the attitude of the drone changes. We use values measured by a motion capture camera system (Prime$^{\mathrm{X}}$22, OptiTrack) as ground truth, and all sensor values are recorded by a ROS program run on an intel-NUC11TNKi7 processor attached to the drone. The drone used in the experiment is shown in Fig. 2.

The configuration parameters are chosen as follows: $q_0 = (-0.136, 0, 0, -0.991), \tilde{V} = 10^{-4} I_3, \tilde{V}_0 = 10^{-2} I_3, \tilde{M}_C = 1.218 \times 10^{-7} I_3, M_C = 1.218 \times 10^{-7} I_4, N_C = 9 \times 10^{-8} I_3, N = 100, J = 100, \Delta t \approx 0.01, K = 1000$. The covariances of process and measurement noises are set to the values inherent to the IMU. In Fig. 3, we present the plots of the actual quaternion components of the attitude of the drone alongside with the estimated values from the filters, as well as a plot of $\hat{d}_k$. All the three filters perform well in estimating attitude tendencies, although the estimates from PF occasionally exhibit greater deviations from the actual values than the

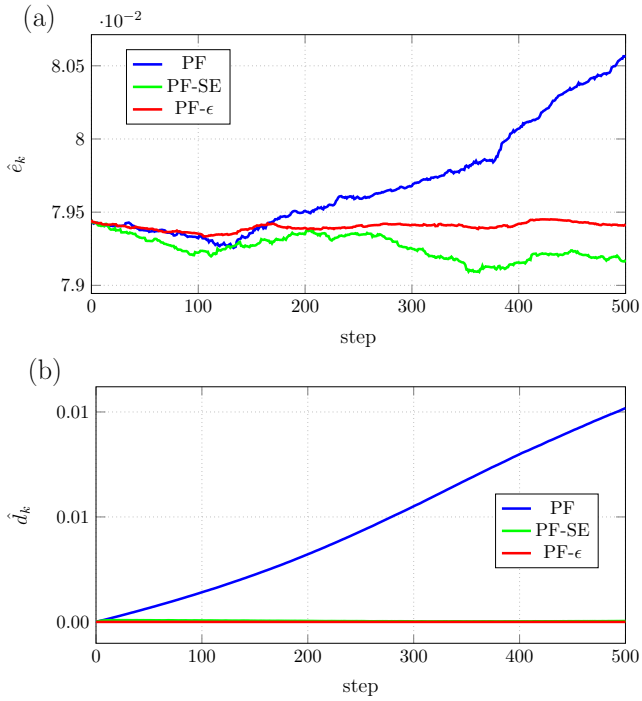

Fig. 1: (a) Estimation error and (b) distance from S^3 of filters in simulation.

TABLE I: Average error, distance from S^3, and computation time of the filters in simulation.

	$[\hat{e}_k]$	$\left[\hat{d}_k\right]$	computation time[ms]
PF	0.07970	4.62882×10^{-3}	1.60459
PF-SE	0.07926	4.56059×10^{-5}	1.66216
PF-ε	0.07940	2.57944×10^{-18}	4.02403

Fig. 2: The drone used in the experiment and the system called FFT-GYRO 450 which restricts the drone to rotational motion

other filters. Both PF-SE and PF-ε provide accurate attitude estimations, with PF-SE demonstrating the lowest $[\hat{e}_k]$, as indicated in table II. Fig. 3(b) illustrates that, similarly to the simulation results, PF-SE maintains its proximity to S^3 even as steps progress, while PF gradually deviates. In Table II, it is evident that PF-SE achieves a value of $[\hat{d}_k]$ approximately 76.03 times smaller than that of PF. As in the simulation results, PF-SE and PF-ε require 1.04 and 2.5 times more computation time than PF, respectively.

TABLE II: Average error, distance from S^3, and computation time of the filters in real drone experiment.

	$[\hat{e}_k]$	$[\hat{d}_k]$	computation time[ms]
PF	0.21063	6.26752×10^{-2}	1.49577
PF-SE	0.18347	8.24322×10^{-4}	1.55660
PF-ε	0.18401	1.76792×10^{-18}	3.73361

We investigate the effect of the number of particles on the performance and computation time, as shown in Fig. 4, where we repeated the experiments with different numbers of particles as $\{20, 50, 100, 200, 500, 1000, 2000\}$. PF-SE consistently demonstrates the lowest values of $[\hat{e}_k]$, while PF exhibits the poorest performance across all conditions in Fig. 4(a). Concerning computation time, as depicted in Fig. 4(b), PF boasts the shortest computation time, while PF-SE and PF-ε require about 1.05 and 2.59 times more time than PF, respectively. Although it is well-known that the performance of particle filters improve with an increased number of particles, the gap in error differences between the filters persists even as the number of particles increases. Furthermore, PF-SE not only possesses the stability property inherent to S^3, but its computation time is also comparable to that of PF. This allows for the possibility of applying additional techniques for other tasks of the drone or employing more particles to enhance performance compared to PF-ε with the same computational resources.

IV. CONCLUSIONS

In this study, we have introduced a novel approach to enhance the performance of the particle filter for state estimation for the rigid body attitude system evolving on

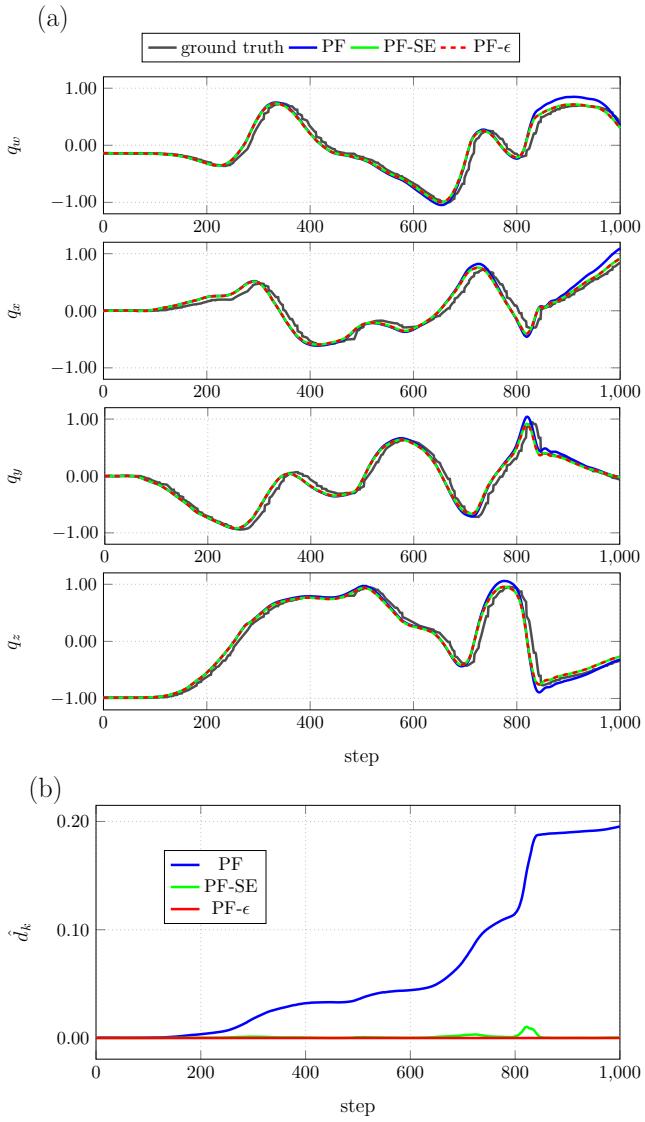

Fig. 3: (a) Plots of the actual and estimated quaternion elements and (b) distance from S^3 of filters in real drone experiment.

the manifold, S^3. Our method incorporates stable embedding into the particle filter, enabling more accurate and efficient state estimation. By extending the original system defined on the manifold to Euclidean space and modifying it to ensure stability on the manifold, we have successfully developed the particle filter with stable embedding.

We have conducted a performance analysis comparing other particle filters. We confirm that our proposed filter not only outperforms the standard particle filter, which directly applies a particle filter designed on Euclidean space, but also provides highly accurate attitude estimation at a lower computational cost compared to a filter that employs techniques to preserve the manifold structure. In practical applications, with our filter it becomes possible to use more particles and represent the distribution of more complex systems while maintaining stability on manifolds under limited

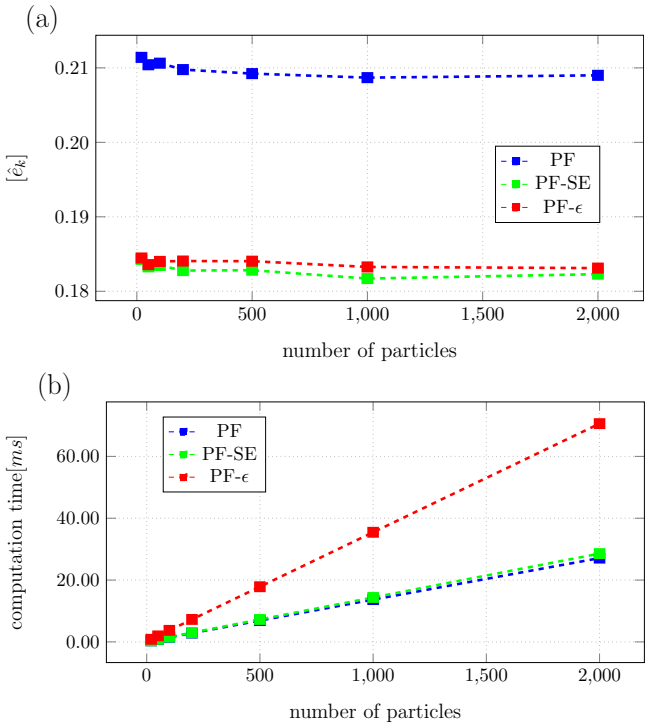

Fig. 4: (a) Average estimation error and (b) computation time of filters according to the number of particles.

computational resources. Moreover, particle initialization and resampling techniques designed to improve performance devised on Euclidean space can be applied directly without any modification, which is another advantage of our filter.

ACKNOWLEDGMENT

The authors would like to thank Dong Hyun Park for his help with the drone experiments.

REFERENCES

[1] W. Ko, K. S. Phogat, N. Petit, and D. E. Chang, "Tracking controller design for satellite attitude under unknown constant disturbance using stable embedding," *Journal of Electrical Engineering & Technology*, vol. 16, pp. 1089–1097, 2021.

[2] J.-H. Park, K. S. Phogat, W. Kim, and D. E. Chang, "Transversely stable extended Kalman filters for systems on manifolds in Euclidean spaces," *Journal of Dynamic Systems, Measurement, and Control*, vol. 143, no. 6, p. 064501, 2021.

[3] J.-H. Park and D. E. Chang, "Unscented Kalman filter with stable embedding for simple, accurate, and computationally efficient state estimation of systems on manifolds in Euclidean space," *International Journal of Robust and Nonlinear Control*, vol. 33, no. 3, pp. 1479–1492, 2023.

[4] M.-D. Hua, G. Ducard, T. Hamel, R. Mahony, and K. Rudin, "Implementation of a nonlinear attitude estimator for aerial robotic vehicles," *IEEE Transactions on Control Systems Technology*, vol. 22, no. 1, pp. 201–213, 2013.

[5] A. Barrau and S. Bonnabel, "Intrinsic filtering on Lie groups with applications to attitude estimation," *IEEE Transactions on Automatic Control*, vol. 60, no. 2, pp. 436–449, 2014.

[6] A. Chiuso and S. Soatto, "Monte Carlo filtering on Lie groups," in *Proceedings of the 39th IEEE Conference on Decision and Control (Cat. No. 00CH37187)*, vol. 1. IEEE, 2000, pp. 304–309.

[7] J. Kwon, M. Choi, F. C. Park, and C. Chun, "Particle filtering on the Euclidean group: framework and applications," *Robotica*, vol. 25, no. 6, pp. 725–737, 2007.

[8] J. Liu and M. West, "Combined parameter and state estimation in simulation-based filtering," in *Sequential Monte Carlo methods in practice*. Springer, 2001, pp. 197–223.

[9] C. Choi and H. I. Christensen, "Robust 3D visual tracking using particle filtering on the special Euclidean group: A combined approach of keypoint and edge features," *The International Journal of Robotics Research*, vol. 31, no. 4, pp. 498–519, 2012.

[10] C. Zhang, A. Taghvaei, and P. G. Mehta, "Feedback particle filter on Riemannian manifolds and matrix Lie groups," *IEEE Transactions on Automatic Control*, vol. 63, no. 8, pp. 2465–2480, 2017.

[11] T. Yang, P. G. Mehta, and S. P. Meyn, "Feedback particle filter," *IEEE transactions on Automatic control*, vol. 58, no. 10, pp. 2465–2480, 2013.

[12] G. Marjanovic and V. Solo, "An engineer's guide to particle filtering on matrix Lie groups," in *2016 IEEE International Conference on Acoustics, Speech and Signal Processing (ICASSP)*. IEEE, 2016, pp. 3969–3973.

[13] G. Marjanovic, M. J. Piggott, and V. Solo, "A simple approach to numerical methods for stochastic differential equations in Lie groups," in *2015 54th IEEE Conference on Decision and Control (CDC)*. IEEE, 2015, pp. 7143–7150.

[14] G. Marjanovic and V. Solo, "An engineer's guide to particle filtering on the Stiefel manifold," in *2017 IEEE International Conference on Acoustics, Speech and Signal Processing (ICASSP)*. IEEE, 2017, pp. 3834–3838.

[15] H. Snoussi and A. Mohammad-Djafari, "Particle filtering on Riemannian manifolds," in *AIP Conference Proceedings*, vol. 872, no. 1. American Institute of Physics, 2006, pp. 219–226.

[16] D. E. Chang, "On controller design for systems on manifolds in Euclidean space," *International Journal of Robust and Nonlinear Control*, vol. 28, no. 16, pp. 4981–4998, 2018.

[17] M. S. Arulampalam, S. Maskell, N. Gordon, and T. Clapp, "A tutorial on particle filters for online nonlinear/non-Gaussian Bayesian tracking," *IEEE Transactions on signal processing*, vol. 50, no. 2, pp. 174–188, 2002.

[18] G. Kitagawa, "Monte Carlo filter and smoother for non-Gaussian nonlinear state space models," *Journal of computational and graphical statistics*, vol. 5, no. 1, pp. 1–25, 1996.

[19] C. Kuptametee and N. Aunsri, "A review of resampling techniques in particle filtering framework," *Measurement*, vol. 193, p. 110836, 2022.

[20] Z. Wang and V. Solo, "Lie group state estimation via optimal transport," in *ICASSP 2020-2020 IEEE International Conference on Acoustics, Speech and Signal Processing (ICASSP)*. IEEE, 2020, pp. 5625–5629.

[21] F. L. Markley, Y. Cheng, J. L. Crassidis, and Y. Oshman, "Averaging quaternions," *Journal of Guidance, Control, and Dynamics*, vol. 30, no. 4, pp. 1193–1197, 2007.

[22] C. J. Bordin Jr, C. G. de Figueredo, and M. G. Bruno, "Nonlinear state estimation on unit spheres using manifold particle filtering," *Digital Signal Processing*, vol. 81, pp. 50–56, 2018.

[23] K. Krakowski, K. Hüper, and J. Manton, "On the computation of the Karcher mean on spheres and special orthogonal groups," in *Conference Paper, Robomat*. Citeseer, Coimbra, Portugal, 2007.

[24] N. Trawny and S. I. Roumeliotis, "Indirect Kalman filter for 3D attitude estimation," *University of Minnesota, Dept. of Comp. Sci. & Eng., Tech. Rep*, vol. 2, p. 2005, 2005.

[25] M. Zamani *et al.*, "Deterministic attitude and pose filtering, an embedded Lie groups approach," Ph.D. dissertation, Australian National University Canberra, Australia, 2013.